The Canadian society for engineering in agricultural, food, and biological systems

CSAE SCGR

La société canadienne de génie agroalimentaire et biologique

Paper No. 05-099

POSITION DETERMINATION USING LANDMARK LOCALIZATION FOR A MOBILE ROBOT

A. Paul, N. Wang, Z. Zhao

[2]Department of Bioresource Engineering, McGill University, 21,111 Lakeshore Sainte-Anne-de-Bellevue, Qc, H9X 3V9, ning.wang@mcgill.ca

Written for presentation at the
CSAE/SCGR 2005 Meeting
Winnipeg, Manitoba
June 25- 29, 2005

Abstract: An artificial landmark-based, automatic navigation system was developed for a small-scale field robot. Several low-cost sensing techniques were involved in the system to detect surroundings and determine the position of the moving robot. Several tests were conducted to evaluate the accuracy of linear distance and angular displacement using dead-reckoning with a gyro-correction, overall performance of the gyroscope used, and effectiveness of an artificial-landmark-based automatic navigation. The accuracy of the position determination methods based on dead-reckoning only, dead-reckoning with a gyro-correction, and laser-range-finder (LRF)-based methods was tested, analyzed, and compared, respectively. The results of the automatic navigation tests showed that LRF-based position estimation was much more accurate when compared to the dead-reckoning and dead-reckoning with gyroscope correction approaches. It had the ability to navigate the testing robot with a high accuracy.

Key words: *Automatic Navigation System, Laser Range Finder, Kalman Filter, Sonar, Dead-Reckoning, Gyroscope Correction*

INTRODUCTION

The concept of the automatic guidance of agricultural vehicles dates back to the early fifties and sixties when leader cable guidance systems were used (Morgan, 1958). As time progressed, various sensing methods for vehicle positioning have been developed. These methods can be placed into two main categories, namely ground-based and satellite-based. Sensors can also be classified in various categories such as motion measurements (odometry and inertial), artificial landmarks (laser and radar), and localisation (sonar sensors and CCD cameras). Ground-based navigational methods can be further subdivided into two schemes, a Cartesian map-based and a relative sensor-based method. A map-based method requires a 2D or 3D model of its operating environment in conjunction with a dead reckoning and motion control system with real time localisation capabilities. A sensor-based navigation method is required to convert 3D structural data into sufficient guidance commands.

Dead-reckoning is a simple technique employed by mobile robots for localization, that integrates the rotation and translation of the contact wheel(s) to calculate the robot's Cartesian coordinates. This method, however, is unreliable because of the accumulation of errors over time as mentioned earlier, thus many researchers believe it is unsuitable for real world applications. However, Yamauchi (1996) claimed that although dead reckoning is insufficiently precise for low-level navigation, it provides general information with respect to the robot's position. The author applied the concept of evidence grid (a region in space divided into Cartesian grid) on a Nomad 200 robot (Nomadic Technologies, California, USA) to compensate for errors arriving from dead reckoning due to slip. The results indicated that this technique produced more accurate position estimation. One major advantage of this method was that it withstood transient changes, such as people walking past the robot and rearrangement of obstacles.

Gyroscopes and accelerometers are two types of inertial sensors that can be used as an alternative for vehicle positioning as oppose to wheel encoders for dead reckoning. They have been used in various vehicle applications (Schonberg et al., 1996). There are three main types of gyroscopes, spinning mass gyros, optical gyros, and vibrating gyros. Spinning mass gyros typically has a mass spinning steadily with a free moveable axis (gimbal). When the gyroscope is tilted, it causes precession, which is the motion orthogonal to the direction of the tilt sensed on the rotating mass axis, so that the angle moved is obtained. In an optical gyroscope, a laser ray is reflected continuously within an enclosure. The enclosure is allowed to rotate and the duration between the time of laser emittance to reception is calculated. Fibre-Optic gyroscope (FOG) is an example of an optical gyroscope that uses a coil of optical fibre. Vibrating gyroscopes, on the other hand, consist of a vibrating element (vibrating resonator chip) that uses the Coriolis effect of the sensor element to sense the speed of rotation. The vibrating element causes secondary vibration orthogonal to the original vibrating direction. The rate of turn is related to the secondary vibration. In Japan, an automated six-row rice transplanter was developed using RTK-GPS for precise positioning and FOG sensors to measure direction (Nagasaka et al, 2004). The RTK-GPS achieved 2 cm precision at 10 Hz data output rate, and the FOG sensors were used to maintain the transplanter inclination. The inclination of the transplanter due to changes in terrain affected the position of the machine, but was corrected using the FOG sensor data. FOG drift was compensated by comparing the lateral direction deviation calculated using the yaw angle and the machine speed with the deviation calculated from the GPS data. An autonomous mobile robot

(AMR) navigation system using a differential encoder and a gyroscope was developed by Park et al (1997). They used an AUTOGYRO (FOG) on a lab-scale mobile robot. Their experimental results demonstrated that the position of the robot was much more precise by combining the encoder and gyroscope readings. The systematic errors arising from the differential encoder and the stochastic errors from the gyroscope were modeled in the navigation filter. An indirect Kalman filter was used instead of an extended Kalman filter, since the indirect method estimated both the errors from the encoder and gyroscope, and by augmenting both of these errors the filter was able to correct them both.

A landmark is localized physical feature that a robot can sense and use to estimate its own position in relation to a known map or a reference frame. The landmark-based navigation is based on detection and recognition of these features in a robot's environment in order to navigate the robot to a specific location. These features can be defined using natural or artificial landmarks. They can also be generated from a known map or geometric models. Natural landmarks are flexible, easy to use and cheap. However, it is often sparse and unstable. Artificial landmarks can be predefined and this tends to reduce the complexity of the localization algorithms. Both natural and artificial landmark-based localization require high performance sensors to accurately detect them. Landmarks can be detected using several sensing mechanisms, including mechanical sensors, sonar sensors, laser scanners, radar, and CCD cameras. However, these sensing methods have their pros and cons. Mechanical sensors were one of the first types of sensors used to detect plant rows, soil furrows, and artificial landmarks such as rails and buried cables, to navigate agricultural field machines. This is a cheap method but accuracy and reliability was very poor. Laser scanners and sonar sensors are also relatively cheap and easy to implement, but they suffer from noise interference, beam spreading and scattering. However, localization using laser scanners to identify artificial landmarks is a promising absolute technique in terms of performance and cost. This technology usually involves the measurement of the bearing of artificial landmarks relative to each other. The position of a robot can be computed using two distinctive techniques: triangulation and Kalman filtering algorithm (Skewis and Lumesly, 1994; Durrant-Whyte, 1996). Visual detection of landmarks using cameras is a rapidly advancing technique (Mata et al, 2003; Hayet et al, 2003; Sala et al, 2004) due to its accuracy and reliability. Visual recognition is the problem of determining the position and orientation of a physical landmark from an image projection of that landmark. This problem poses lots of challenges in real life because of uncontrolled illumination, distances, and view angles to the landmarks, as well as requirement for resources to store and process the image data. The visual detection of landmarks has been based on several fundamental concepts, such as the detection and extraction of *contour segmentation, 2D line segmentation, vertical lines, intersecting lines, edges,* and *vanishing points*.

In practice, cheap and reliable sensing methods are the preferred way. But there is often a trade-off between costs and accuracy. Dead reckoning is unreliable and results in accumulated error over long period of time. The fusion of two or more sensors to predict position and orientation of a mobile robot is also common, but this method requires complex algorithms and models to represent the errors created by the sensors. Localization using artificial or natural landmarks is a common technique because of its simplicity, low cost and reliability.

The primary objective of this study was to develop a landmark localisation technique based on a LRF and artificial landmarks, and to develop an algorithm to improve position estimation for navigational purposes. The specific aims included:

- To test the linear and angular displacement accuracy of the robot using the onboard gyroscope and wheel encoders.
- To test the effectiveness of the combination of the gyroscope and dead reckoning measurements using a Kalman filter algorithm in compensating errors due to slip.
- And finally, to develop a landmark localisation technique using a LRF and artificial landmarks, and to compare it against the inertial measurement method

MATERIALS AND METHODS

HARDWARE DESCRIPTION

The Robot Platform

The automatic navigation system was developed for a Pioneer 3 All Terrain (P3-AT) robot (ActivMedia Robotics, New Hampshire, USA). The robot was equipped with two internal sensors, namely a gyroscope chip (ADXRS300, Analog Devices, Massachusetts, USA) and two wheel encoders used for dead reckoning. Two external sensors included a LRF (SICK LMS200, Waldkirch, Germany) and a ring of eight sonar sensors. The body of the robot was made of aluminium with dimensions of 50cm(L)×49cm(W)×26cm(H) and a body clearance of 8 cm. The total weight was 12 kg including three 12 V batteries. It was four-wheel driven (21.5 cm diameter drive wheels), employing a skid steering approach for turning. The wheel motors used a 66:1 gear ratios and contained two 100-ticks wheel encoders. The maximum translational speed that could be achieved was 1.2 m/s and the maximum traversable slope was 40 % grade.

The P3-AT robot was also equipped with an 850 MHz single-board computer (VSBC8, VersaLogic Corporation, Oregon, USA), and an 18 MHz microcontroller (H8S/237, Hitachi, Japan). The microcontroller managed all the low-level details of the robot's control and operation, including motion, heading and odometry. The single-board computer was used to acquire and process LRF data in real-time and implement the automatic navigation algorithms.

Internal Positioning Sensors

The gyroscope (ADXRS300, Analog Devices, Massachusetts, USA) used was an angular rate sensor built using proprietary MEMS®surface micromachining process by Analog Devices. It had a dynamic range of ±300 °/sec and a sensitivity of 5 mV/°/sec. The bandwidth was 0.04 kHz and the temperature range was -40°C to 85 °C. The power supply and current requirement were 4.75 V and 6 mA respectively.

The purpose of the gyroscope was to compensate for large errors due to wheel slip, lost of wheel contact on the ground, and other factors like skid steering and gearbox play. The gyroscope was connected to an analog to digital input port on the microcontroller. Gyroscope measurements were of 10 bit integers of value 0-1023. When the robot was stationary the measurement was centered around 512. Measurements less than 512 represented counter-clockwise direction and measurements above 512 represented clockwise direction. The measurements were dependant on

the gyroscope's temperature and drift. In the event of drift, the gyro auto calibrated itself to the centre range of 512 if the robot was stationary for one second. A stationary position meant the rotational and translational velocities were less than 1 °/sec and 1 mm/sec respectively for a period of 1 second. Another condition for auto calibration to take place was that the gyro's current reading must be within 0.5% of the average readings.

The P3-AT robot had four wheel motors and two wheel encoders. The two left-wheel and two right-wheels were mechanically coupled (with a belt) respectively, thus the encoders produce two distinct speeds, one for the left pair and the other for the right pair. The dead reckoning concept used consisted of simple geometric equations using odometric data to calculate the position of the robot in comparison to its starting point. The dead reckoning concept is shown below:

X_1-Y_1: Local coordinate frame
X_2-Y_2: Global coordinate frame

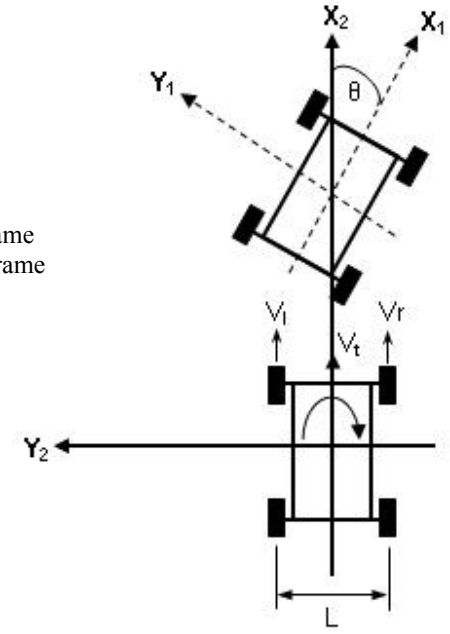

Figure 1. Dead Reckoning Concept

Figure 1 shows the robot after undergoing a translational and rotational movement. X_2-Y_2 was considered as a global coordinate frame and X_1-Y_1 as a local coordinate frames of the robot. V_l and V_r represented the left and right encoder velocities respectively, whilst V_t was the total translational velocity. The robot's heading was represented as an angle θ, with an angular velocity as $\dot{\theta}$. V_t was resolved into two components of velocity, a horizontal and vertical components. The Cartesian coordinates of displacement was obtained by an integration of the horizontal and vertical components of translational velocity over time. The distance measurement was computed using equations 1 to 5.

$$V_t = \frac{V_r + V_l}{2} \qquad (1) \qquad V_r = V_t + \frac{L\dot{\theta}}{2} \qquad (2)$$

$$V_l = V_t - \frac{L\dot{\theta}}{2} \qquad (3) \qquad \dot{\theta} = \frac{V_r - V_l}{L} \qquad (4)$$

$$x = \int_0^t v_x \, dt \qquad (5) \qquad y = \int_0^t v_y \, dt \qquad (6)$$

Where:

V_l – left encoder velocity
V_r – right encoder velocity
L – distance between left and right encoder
θ – angle between X_1 axis and X_2 axis
$\dot{\theta}$ – angular velocity in the *x-y* plane
x – vertical displacement
y – horizontal displacement

LRF and Sonar Sensors

The LRF operated on the principle of "time of flight" measurements. The field of view was 180°, and the maximum measurement range was 150 m. The angular resolution was selected at 0.5° by means of the software. The statistical error of the LRF was ± 15 mm for distances of 1 m to 8 m, and ±4 cm for distances of 8 m to 20 m. The advantages of using a LRF as a navigation and localization sensor were its high scanning frequency (75 Hz) and the transfer of measurement data to the single-board computer occurred in real-time.

A total of eight sonar sensors were mounted on the robot. The sensitivity and range of the sonar sensors were adjusted using a gain control adjuster located under the robot's panel. An appropriate setting was used depending on the environment in which the robot was working. Low-gain settings reduced the robot's ability to detect small obstacles, therefore, was useful when operating in noisy environments, or on uneven or highly reflective surface. As the sensitivity, the sonar sensors were able to detect smaller obstacles and objects at a distance further away. Each sonar sensor were multiplexed and the acquisition rate of the array was 25 Hz (40 milliseconds per sonar array)

SOFTWARE DESIGN

The overall software structure consisted of two parts, a low-level control operating system running on the microcontroller, and an autonomous navigation and localization program running on the single-board computer. ActivMedia Robotics Operating System (AROS) was running on the microcontroller (server) and ActivMedia Robotics Interface Application (ARIA) was running on the single-board computer (client). The microcontroller communicated with the single-board computer using special client-server communication packet protocols over a RS-232 interface. The server information packet (SIP) contained information about the sonar sensors measurement, gyroscope measurements, and odomteric measurements. ARIA was used to decode and interpret the information in the SIP and to send appropriate commands to the wheel motors for motion control.

The ARIA program that was developed comprised basically of two threads; a LRF thread, which was used primarily for receiving and processing data from the LRF and a main thread, which performed a variety of functions for planning, and intelligent, purposeful control of the robot's platform and its components (Figure 2 (a)). The main thread consisted of eleven functions and was executed every 100 ms (Figure 2 (b)). This included functions for interpreting and analyzing the encoder and gyroscope readings encoded in the SIPs from the microcontroller by the Packet handler (1). The key handler (6) was used for interfacing the keyboard with ARIA for setting and changing modes of operations of the robot by pressing an appropriate key on the keyboard. Various modes such as automatic and manual operation were developed for testing and

evaluating the robot. Appropriate keys on the keyboard were defined to allow the selection of the operation mode. The keyboard also served as a means of entering file names for data storage and for setting target coordinates manually for the robot. The function action handler (8) executed the tasks of obstacle detection, obstacle avoidance and all motion such as forward, reverse, and turns. The motion commands sent by the single-board computer was used to control the mobility of the robot, e.g. to set individual wheel speeds, or coordinated translational and rotational velocities; to change the robot's absolute or relative heading; to move the robot to a specific distance or; to stop the robot.

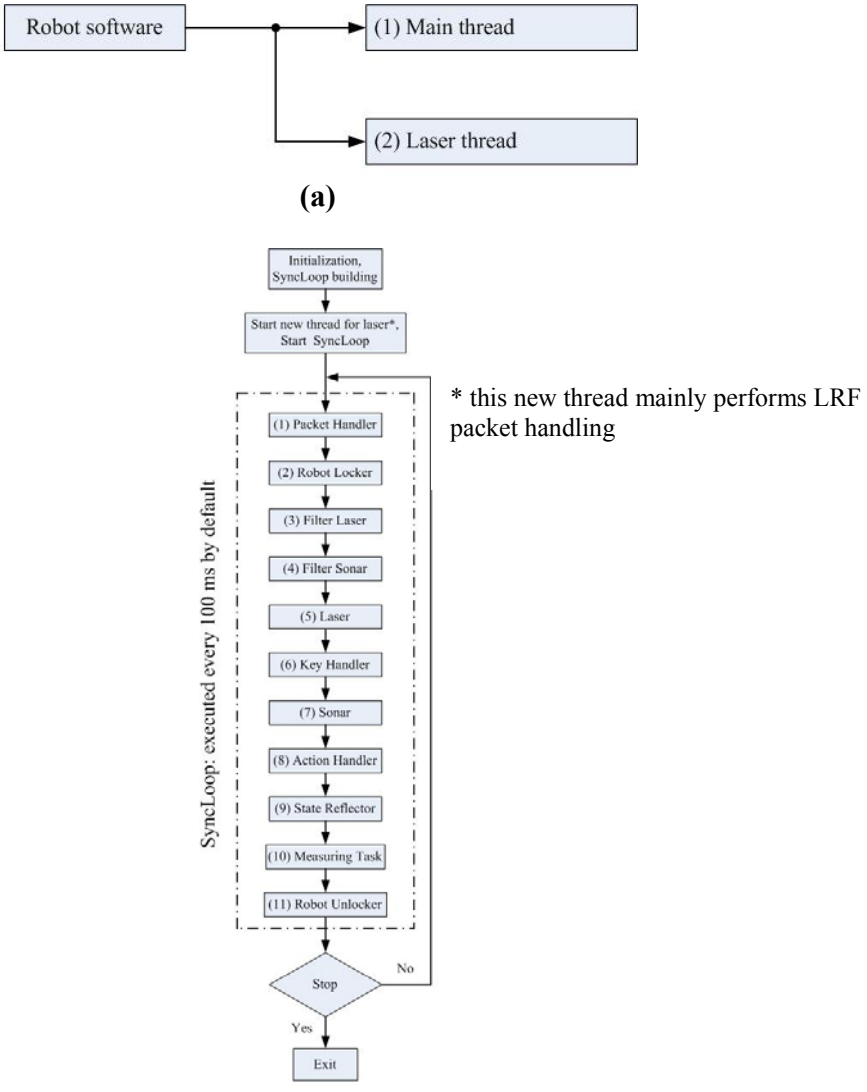

Figure 2. Block Diagram of the Software Structure

With respect to localization using artificial landmarks, the LRF was included in the software to detect two landmarks (two cylindrical poles) and the appropriate equations were developed to compute the Cartesian coordinates of the robot relative to the poles, and finally these coordinates were transformed unto the global coordinate system.

Results from the wheel encoders, gyroscope and LRF were collected every 100 ms and written to a data file for analysis.

Kalman Filter

When using more than one sensor modality to obtain position orientation, such as a gyroscope and wheel encoders, an algorithm is needed to combine the readings to produce an accurate estimation of position. Typically a Kalman filter is used for this purpose. There are two main types of Kalman filters, the extended Kalman filter (also known as the direct Kalman filter) and indirect Kalman filter. The extended Kalman filter (EKF) does not correct the systematic encoder errors and gyroscope errors mutually, but merely minimize their errors using independent models. The indirect Kalman filter estimates the systematic errors of the encoders and the stochastic errors of the gyroscope exclusively and is fed back into the navigation system. In this case, the filter is not in the navigation loop but in the case of the EKF the filter is in the main navigation loop. Since the filter is out of the navigation loop with respect to the indirect approach, the encoder information will be available even if the filter fails or if it not used (Park et al, 1997).

An indirect Kalman filter was used in this research. The Kalman filter was outside the main navigation loop. The encoder information was available even if the Kalman filter was not used. A block diagram is shown in Figure 3.

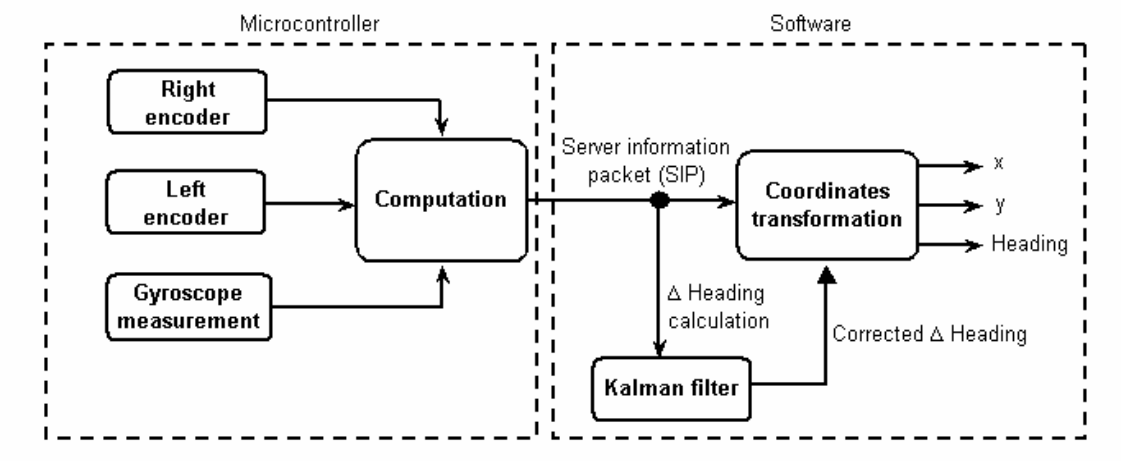

Figure 3. The Kalman Filter in the Automatic Navigation System

The microcontroller computed the position and orientation of the robot with data from the gyroscope and right and left wheel encoders. The computed position information were then encoded in separate SIPs, and sent to the single-board computer. The single-board computer decoded the SIPs to obtain an estimate of the robot's position and then transformed the readings into a global coordinate frame. The coordinate transformation included transformation of the heading and Cartesian coordinates from a local coordinate frame to a global coordinate frame. When desired, the software was also used to compute only the measurements from the wheel encoders, or the gyroscope, or a combination of the wheel encoders and gyroscope. Considering the latter case using a combination of the gyroscope and encoder readings, a simple Kalman filter

was used. The single-board computer used the information in the relevant SIPs to calculate the final pose of the robot.

SYSTEM TESTS

Several experiments were conducted with the P3-AT robot to gather data about the accuracy of the dead-reckoning method and the effectiveness of the gyroscope. All experiments were carried out indoor on a concrete surface on which a grid was outlined of size 6 m × 6 m consisting of cells 1 m × 1m. With the marked grid, actual distances could be measured quickly and easily. Two cylindrical poles with diameters of 8 cm and 12.5 cm were used for the landmark localisation technique described later. In some instances the robot was programmed to automatically drive to a goal and in other cases it was manually driven to achieve an X,Y coordinate with a specific final heading.

Test 1: Accuracy of linear distance and angular displacement measurements.

Objectives: (1) To determine the effectiveness of combining a gyroscope and dead- reckoning measurements for position estimation when a robot moved in the X direction only without any changes in its Y coordinate
(2) To determine the effectiveness of combining a gyroscope and dead- reckoning measurements for heading when a robot was rotated on a specified spot

Approach: The robot was programmed to automatically drive from it's starting position (0,0,0 in the global frame) to desired distances of 1 m to 10 m in 1 m increment. Distances of 1 m interval were marked on the floor. The robot's final position at each incremental value was noted by making a mark on the ground corresponding to the front wheel centre of the robot (the wheel centre was used as a benchmark). This distance was then measured and recorded. The test was conducted two times, first without using the gyroscope (dead-reckoning only), and secondly with dead-reckoning using gyroscope correction. The measured values for each method were recorded. The test was repeated three times and the average of the measurements were used for analysis.

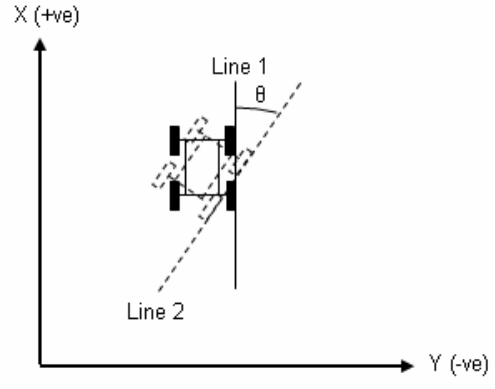

Figure 4. Angular Test Layout

The robot was also programmed to rotate on a spot at desired angles. In order to measure the actual angle turned by the robot, a straight line was drawn on the ground (line 1), and after the robot had rotated a second line was drawn (line 2). The angle turned (θ) was measured, as illustrated in Figure 4. The angular test was conducted in a similar manner as the linear displacement test, with dead-reckoning only and dead-reckoning with gyroscope correction.

The percentage error was computed to evaluate the dead-reckoning and dead-reckoning with gyroscope correction methods, using the expression below:

$$\text{Percentage error} = \left| \frac{\text{Desired distance (angle)} - \text{Measured distance (angle)}}{\text{Desired distance (angle)}} \right| \times 100\%$$

Test 2: Accuracy of position determination on a grid layout.

Objective: To determine the effectiveness of the combined gyroscope and dead reckoning measurements with changes in X,Y coordinates and heading angles

Approach: The robot was manually driven (approximately 300mm/s) to selected points on the grid. In this case, the centre of the robot (from where all positions were defined) was used as a benchmark. At its final position the centre of the robot was aligned to the intersection of the grid lines. A visible mark on the robot's centre allowed for an easy alignment of its centre. The final heading for grid locations 1 to 8 was manually set at +90° and the final heading for grid location 9 to 16 was set at -90°. This was done to maintain consistent motion pattern for all the selected points. When the robot reached its final position, the wheel encoder readings (dead-reckoning only), and the dead-reckoning with gyroscope correction readings were recorded. The percentage error between the actual position and measured positions were computed. The measured position refers to the wheel encoder measurement, and the combined wheel encoder and gyroscope measurement. The percentage error was computed as follows:

$$\text{Percentage error} = \left| \frac{\text{Actual distance} - \text{Measured distance}}{\text{Actual distance}} \right| \times 100\%$$

Test 3: Gyroscope performance during maximum slip.

Objective: To evaluate the performance of the gyroscope during maximum slip (100%)

Approach: The robot was suspended so that the four wheels were not in contact with the ground. It was then "driven" manually (approximately 300 mm/s) for a period of time so that sufficient data was collected and stored in a data file. The robot was "driven" in the forward, reverse, left and right turn directions. In this case, the wheel encoders could not sense that the robot was not physically moving when suspended, but the gyroscope was able to sense this condition. Three types of data were collected, namely, wheel encoder readings, gyroscope readings, and the combined gyroscope and wheel encoders reading. The data was collected every cycle of 100 ms time duration. Data from every 3 cycles were analyzed, and a total of 97 cycles were required as it was the equivalent of a 360° rotation.

Test 4: Landmark localization method for position determination in a grid layout

Objectives: (1) To develop a landmark localization technique using a LRF and artificial landmarks

(2) To evaluate and compare the localization technique developed in (1) with the fusion of sensory readings from the encoders and gyroscope

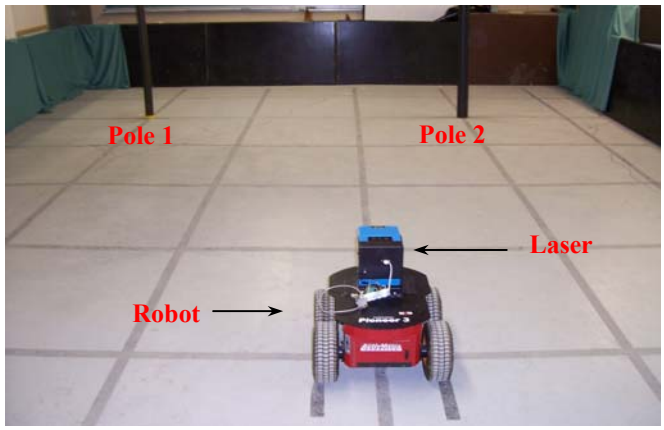

Figure 5. Test Setup for the Landmark Localization Method

Approach: Figure 5 shows the experimental setup. Two poles (used as artificial landmarks) were placed at coordinates of (4000, 2000) and (4000,-1000), respectively, with reference to the robot's global coordinate frame.

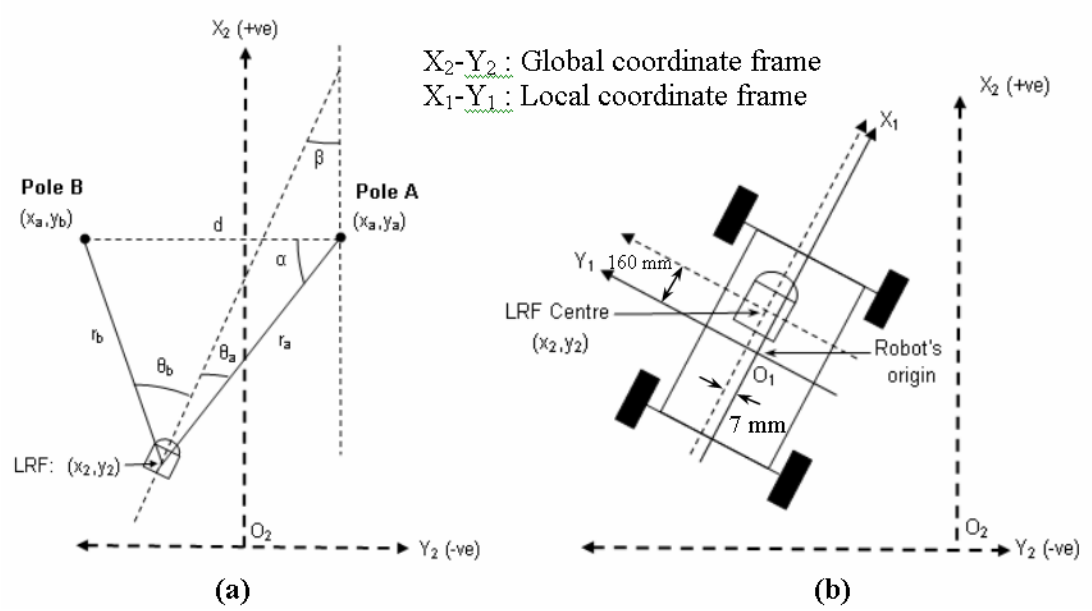

Figure 6. The Artificial Landmark Localization Method

The separation of the landmarks represented as d was set at 3 m in the tests. The distance d could be varied depending on the work space available and the environment in which the robot was working. The distances between the landmarks and the centre of the LRF were defined as r_a and r_b for Pole A and Pole B respectively. θ_a and θ_b were defined as the angles between X_1 axis of the local coordinate frame and the "line of sight" of the poles. In Figure 6 (a), θ_a was defined as a negative angle, and θ_b as a positive angle. Objects detected to the left were assigned a positive value and to the right negative values. The variables r_a, r_b, θ_a and θ_b were all known from the LRF data (Figure 5.6 (a)). In order to compute the position of the LRF (x_2,y_2) with respect to the poles the following equations were derived and used in the landmark localization algorithms.

$$(x_2 - x_a)^2 + (y_2 - y_b)^2 = r_b^{\,2} \quad (7)$$

$$(x_2 - x_a)^2 + (y_2 - y_a)^2 = r_a^{\,2} \quad (8)$$

$$(2y_2 - y_a - y_b) \times (y_b - y_a) = r_a^{\,2} - r_b^{\,2} \quad (9)$$

$$y_2 = \frac{r_a^{\,2} - r_b^{\,2}}{2(y_b - y_a)} + \frac{y_a + y_b}{2} \quad (10)$$

$$x_2 = x_a \pm \sqrt{r_a^{\,2} - (y_2 - y_a^{\,2})} \quad (11)$$

The heading angle β was calculated using the following expressions:

$$\frac{\sin\alpha}{r_a} = \frac{\sin(\theta_b - \theta_a)}{d} \quad (12)$$

$$\sin\alpha = r_b \times \frac{\sin(\theta_b - \theta_a)}{d} \quad (13)$$

$$\beta = 180 - (90 - \theta_a + \alpha) \quad (14)$$

$$\beta = 90 + \theta_a - \alpha \quad (15)$$

Figure 6(b) shows the position of the LRF relative the robot's local coordinate frame. The centre of the LRF was located at 160 mm,7 mm with respect to the local coordinate frame of the robot. The position of the centre of the LRF was subsequently transformed to the robot's origin to obtain the position of the robot in the global coordinate frame.

The robot was again driven to specific locations on the grid and the encoder, gyroscope and landmark localization system readings were all recorded and analyzed.

RESULTS AND DISCUSSION

TEST 1: ACCURACY OF LINEAR DISTANCE AND ANGULAR DISPLACEMENT MEASUREMENTS.

When the robot was driven, the encoder readings were used to calculate its position and orientation. The gyroscope was also activated and changes in headings were recorded. A Kalman filter was used to incorporate the encoder values and gyroscope readings to compute the final position of the robot.

Linear displacement

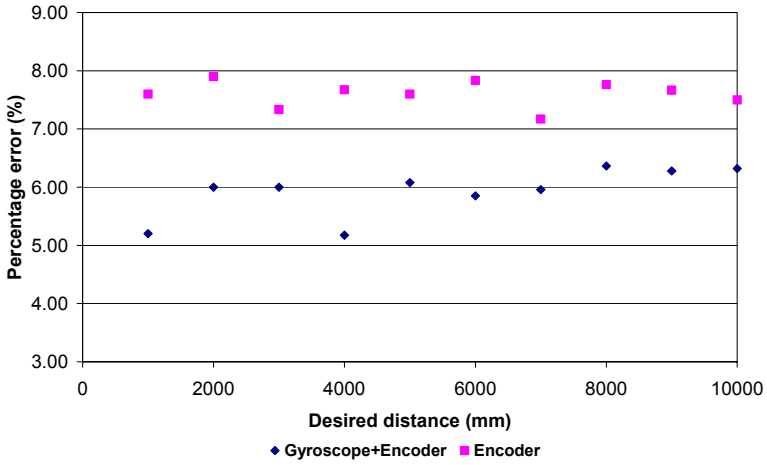

Figure 7. Percentage Error Between Desired and Measured Distances

In Figure 7, the percentage errors between the desired distances and encoder readings varied from a minimum value of 7.17% to a maximum of 7.90% without gyroscope correction. The mean of the percentage errors was 7.60%. On the other hand, the percentage error between the desired distances and the encoder readings with gyroscope correction varied from a minimum of 5.18% to a maximum of 6.36%. The mean percentage error was 5.92%. Obviously, a difference of 1.68% percentage error between the dead-reckoning method and dead-reckoning with gyroscope correction. The dead reckoning system would normally have larger errors over a long period of time. With respect to short distances, the dead reckoning method was reliable. Preliminary tests on the robot had indicated that the percentage errors obtained from the dead reckoning method varied from 20% to 30% for a period of time ranging between 5-15 minutes. This was much larger than the 7.60% as was obtained and can be attributed to the fact that there was no change in the robot's heading and the experiment was not conducted over a long period of time.

Angular displacement

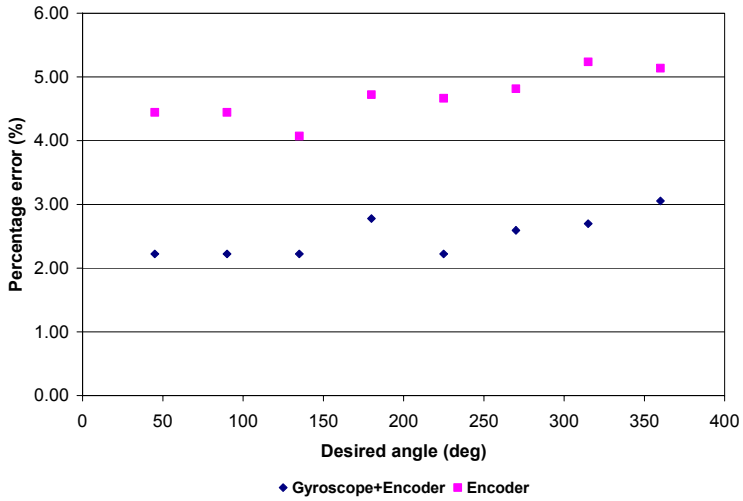

Figure 8. Percentage Error Between Desired and Measured Angles

The results from the angular displacement test is shown in Figure 8. The results indicate that the average percentage error between the desired angle and the measured angle computed using dead-reckoning with gyroscope correction was 2.50%. However, the average percentage error between the desired angle and the angle calculated form the encoder dead-reckoning approach was found to be 4.69%. Figure 8 illustrates that the percentage errors using the combination of the two sensors was much lower than those with just the encoder readings.

TEST 2: ACCURACY OF POSITION DETERMINATION ON A GRID LAYOUT.

This experiment was conducted on a grid layout for the P3-AT robot with changes in both heading and X-Y coordinates. The robot started from position (0,0) and traveled to the 19 locations respectively. Grid position 1 to 16 were all set at a fix X coordinate value of 4000 mm and the heading was set at +90 for locations 1-8 and -90 for locations 9-16.

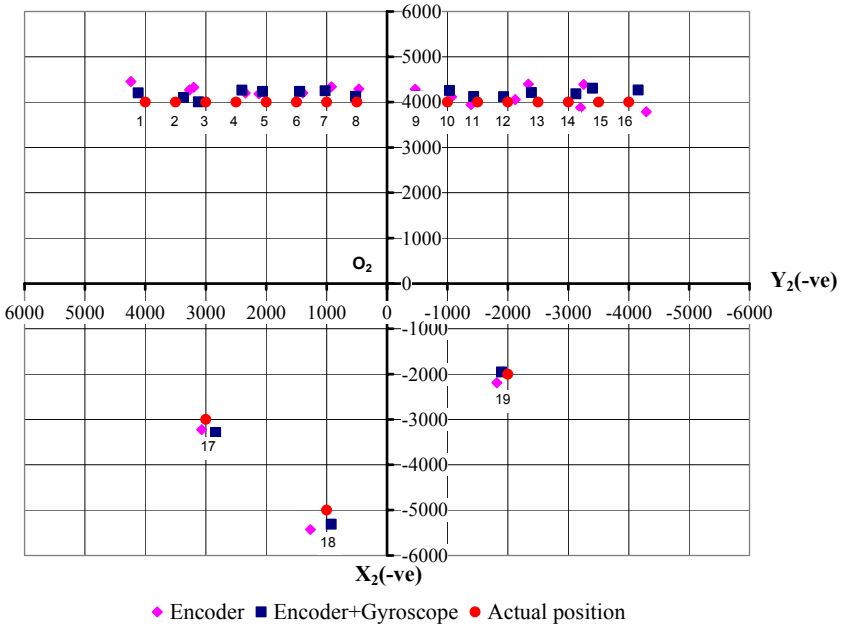

Figure 9. Comparison among Robot's Actual Position, Position from the Encoder, and Position from Encoder with Gyroscope Correction (units in mm)

The test results are shown Figure 9, on a global coordinate frame (X_2,Y_2). The data obtained from dead-reckoning with gyroscope correction were in closer proximity to the actual position of the robot.

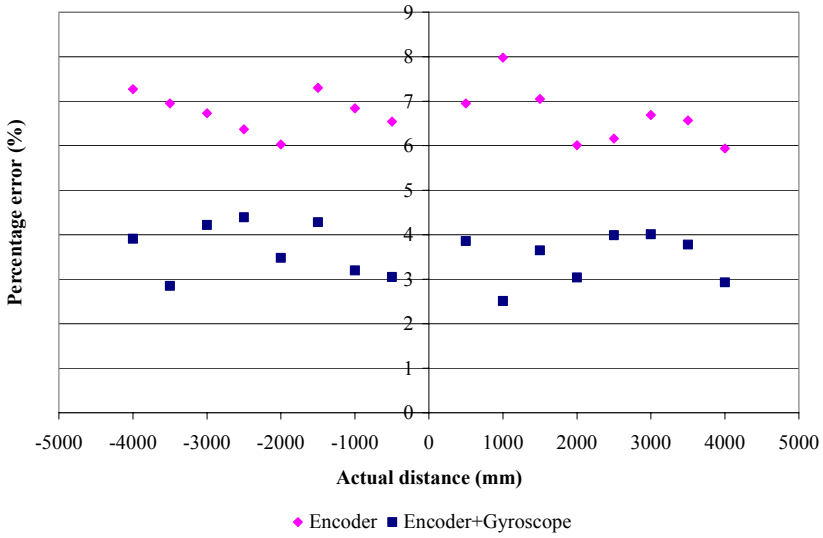

Figure 10. Percentage Error Between Measured and Actual Distances (1-16)

Figure 10 shows the percentage errors for the gird locations 1-16. The encoder readings when compared to the actual position of the robot had a percentage error that varied between 5.94% and 7.98% (mean=6.71%) whilst the position estimation using dead-reckoning with gyroscope correction ranged from 2.51% to 4.39% (mean=3.57%). This was a difference of 3.14% between the two methods, compared to a difference of 1.68% obtained in Test 1. The reason for the large difference was that in this experiment there were changes in the X,Y coordinate as well as the heading. This incurred a higher percentage of errors in the encoder readings.

TEST 3: GYROSCOPE PERFORMANCE DURING MAXIMUM SLIP.
This test was conducted at an average rotational speed of 37 mm/s with the wheels suspended off the ground, whilst the robot was driven manually.

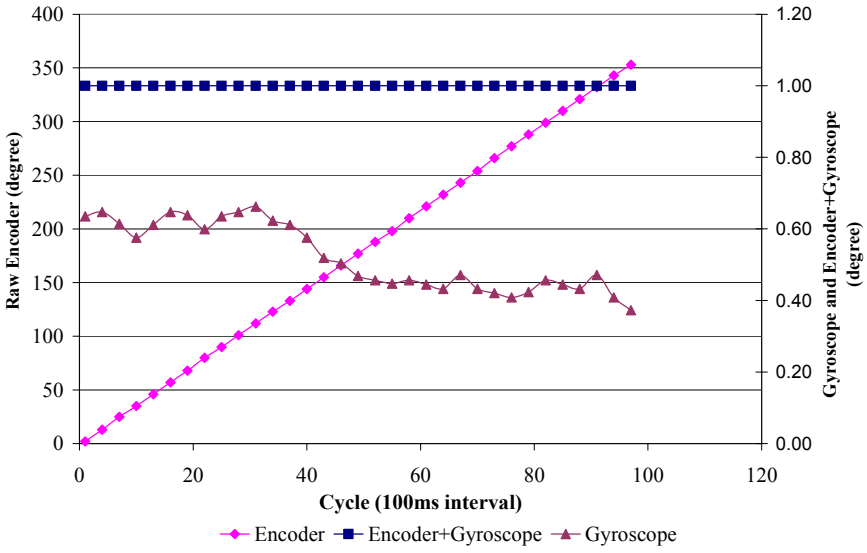

Figure 11. Gyroscope Correction

As time increased the encoders recorded a change in heading calculated from its dead- reckoning approach. The change in heading was quite consistent, resulting in a straight line since the rotational velocity was kept constant. The gyroscope readings according to Figure 11 fluctuated between 0.4° and 0.6°. This may have been caused by a drift due to temperature changes. Although the gyroscope had a temperature sensor to compensate for the drift, other factors such as vibration and the accuracy of the gyroscope could be attributed to this fluctuation in readings. When the encoder and gyroscope readings were fused together the resulting heading was computed as 1°. This was constant for the data examined during this time period of the experiment.

TEST 4: LANDMARK LOCALIZATION METHOD FOR POSITION ESTIMATION IN A GRID LAYOUT

In this test the robot was manually driven to fixed locations on the grid as show in Figure 12. This was very much similar to the experiment described in Test 2 with the exception that the system now comprised of a landmark localization component to ascertain position and orientation. Eighteen grid locations were selected, and the X,Y coordinates and heading angles were all recorded.

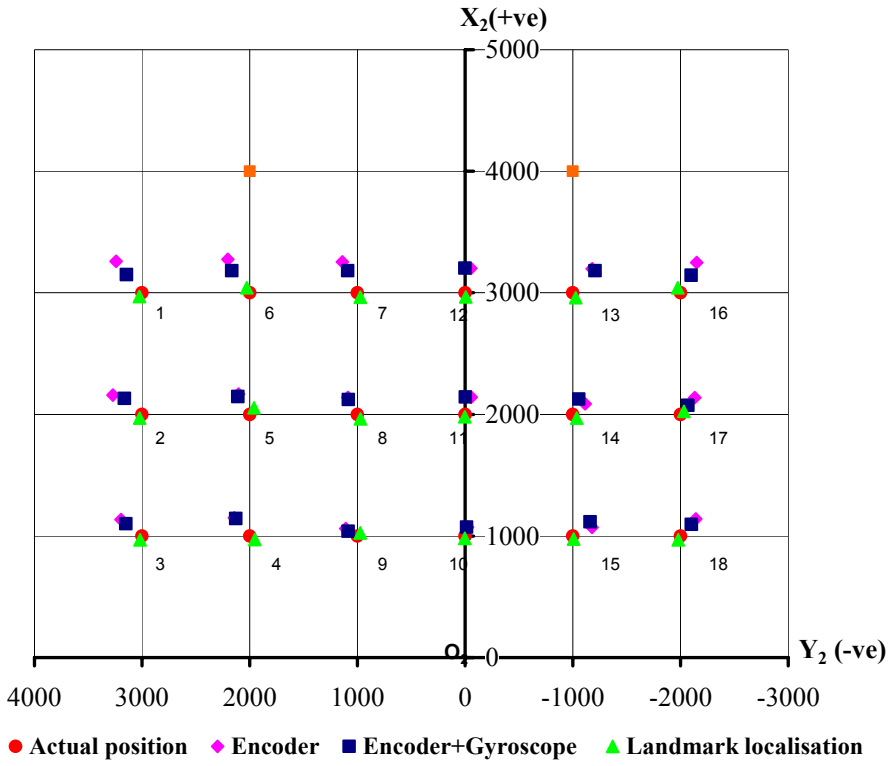

Figure 12. Results from the Artificial Landmark Localization Method (units in mm)

Figure 12 illustrates the final X and Y coordinates of the robot on the grid determined by the encoder, encoder with gyroscope correction, and the landmark localization measurements, respectively. The landmark localization technique lay in the closest proximity to the actual position of the robot.

Analysis of all the data from this test showed that there was a significant increase in the accuracy of the position computation using the landmark localization technique. The mean percentage error between the actual and measured values for the landmark localization method for the X and Y coordinates were 1.95% and 1.93% respectively. The percentage error for the X and Y coordinates with the encoder readings was 8.59% and 10.38% respectively, whilst with the encoder with gyroscope correction was 6.80% and 7.93% respectively. This translates to within 2-3.5 cm accuracy for the landmark localization method with respect to the actual positions employed in this experimental layout.

Table 1. Summary of Percentage Errors

Position estimation method	Percentage error (%)	
	x	Y
Dead reckoning	8.59	10.38
Dead reckoning with gyroscope correction	6.8	7.93
Artificial landmark localization	1.95	1.93

In summary, the landmark localization method based on a LRF offered the most accurate estimation of position and orientation (Table 1). The LRF was used to determine: 1) the distances and angles of the landmarks relative to the robot and 2) to compute the position and orientation of the robot in a global coordinate frame. Dead-reckoning on the other hand, could be very reliable for short distances and environments with minimum slip. However, as time increases, the errors using only the encoders tend to accumulate. This problem is overcome by use of the localization technique, which was not affected by the conditions in which the robot was expected to work (i.e. surface undulation and slippery environments). The accuracy and resolution of the LRF (or any other localization sensor such as a CCD camera or sonar sensor) were the limiting factors that influenced the accuracy of the position estimations.

It must be noted that in this experiment the landmarks (two poles) were placed at the same X coordinate in the reference frame and the LRF on the robot had to be able to detect these two poles simultaneously in order to compute its position and orientation. If the poles were not detected, the resulting position computation produced an error. This was a setback as the motion and path of the robot would be limited and would be impractical and unsuitable for real world applications. This disadvantage could be overcome by placing several known landmarks around the robot's working environment, thereby allowing the robot much more flexibility and path planning capabilities. The onboard gyroscope was a single axis device that detected the yaw rate. This worked satisfactorily as only heading changes were required. In events of undulating terrain, a three-axis gyroscope would be very useful, as slopes can be detected, thus speed and direction could be corrected based on information received from the gyroscope. Overturn of tractors is a very common mishap in agricultural operations resulting in loss of time, money and even harmful to the operators. In the case of an autonomous navigation system safety is of paramount importance, therefore slope detection is crucial and should be incorporated into the control system.

The use of odometric measurements for navigational purposes poses a few challenges in agricultural operations due to a number of factors. First of all, the mere nature of dead- reckoning technique requires a wheel to be in contact with the ground and any changes in the rolling circumference would induce some errors in the position of the vehicle. Considering the conditions in a typical agricultural field with high soil moisture content and the adhesive properties of soil, it is quite natural that at some times soil will stick to the tires on the wheel and in effect increase the rolling radius. The fusion therefore of sensory data seems like a feasible solution as was employed in the navigation system. A Kalman filter can be used to fuse data from the encoders and a gyroscope to improve the accuracy of the position and orientation estimate of the vehicle.

CONCLUSIONS

An indirect Kalman filter was used to fuse dead-reckoning and gyroscope measurements to produce an estimate of a mobile robot's position and orientation. Results from the test showed that the improvements made by the encoder readings with gyroscope correction when compared to only dead- reckoning method was not very significant as the encoder readings tend to be reliable for short distances and also slip was minimal.

A landmark localization technique for computing position and orientation of a mobile robot was successfully developed and tested in an indoor environment. Two artificial landmarks were placed at known positions with respect to the global coordinate frame of the robot. A LRF was used to detect the positions of the two landmarks. The distances of the landmarks from the centre of the LRF were determined using range information. The angles between the line of sight of the landmarks and the X_1 axis of the local coordinate frame were also computed. Suitable equations were derived and included in the localization algorithm to compute the position and orientation of the robot in a global coordinate frame. The results from the tests showed that the position estimation using this technique was much more accurate when compared to the dead-reckoning and dead-reckoning with gyroscope correction approaches. The percentage errors between the actual positions and the computed positions for the X and Y coordinates were found to be 1.95% and 1.93% respectively. This percentage error was significantly less when compared to the percentage errors obtained from the dead-reckoning with gyroscope correction measurements. This was a difference of 4.58% and 6.0% for the X and Y coordinates respectively between the two methods. This was a significant difference due to the fact that the landmark localization method using the LRF was not dependent on the operating environment such as slip and undulation.

REFERENCES

Barshan, B., and H.F. Durant-Whyte. 1994. Orientation estimate for mobile robots using gyroscopic information. *Proceedings of the IEEE/RSJ/GI International Conference on Intelligent Robot and Systems (IROS '94)*. Vol. 3, 1867-1874.

Betke, M., and L. Gurvits. 1997. Mobile robot localization using landmarks. *IEEE Transaction on Robotics and Automation*. Vol. 13 (2), 251-263.

Borenstein, J., and L. Feng. 1996. Measurement and correction of systematic odometry errors in mobile robots. *IEEE Transaction on Robotics and Automation.* Vol. 12 (6), 869-880.

D'Orazio, T., F.P. Lovergine, M. Ianigro, E. Stella, and A. Distante. 1994. Mobile robot position determination using visual landmarks. *IEEE Transactions on Industrial Electronics*. Vol. 41 (6), 654-662.

Durrant-Whyte, H.F. 1996. An autonomous guided vehicle for cargo handling applications. *International Journal of Robotics Research*. Vol. 15 (5).

Hague, T., J.A. Marchant, and N.D. Tillett. 2000. Ground based sensing system for autonomous agricultural vehicles. *Computer and Electronics in Agriculture*. Vol. 25 (1/2), 11-28.

Hayet, J.B., F. Lerasle, and M. Devy. 2003. Visual landmarks detection and recognition for mobile robot navigation. *Proceedings of the IEEE Computer Society Conference on Computer Vision and Pattern Recognition*. Vol. 2, 313-318.

Leonard, J.J., and H.F. Durant-Whyte. 1991. Simultaneous map building and localization for an autonomous mobile robot. *Proceedings of the IEEE International Conference on Intelligent Robots and Systems.* Vol. 3, 1442-1447.

Mata, M., J.M. Armingol, A. De La Escalera, and M.A. Salichs. 2003. Using learned visual landmarks for intelligent topological navigation of mobile robots. *Proceedings of the IEEE International Conference on Robotics and Automation*. Vol. 1, 1324-1329.

Morgan, K.E. 1958. A step towards an automatic tractor. *Farm mech*. Vol. 10 (13), 440-441

Nagasaka, Y., N. Umeda, Y. Kanetai, K. Taniwaki, and Y. Sasaki. 2004. Autonomous guidance for rice transplanting using global postioning and gyroscopes. *Computer and Electronics in Agriculture*. Vol. 43 (3), 223-234.

Park, K., H. Chung, J. Choi, and J.G. Lee. 1997. Dead reckoning navigation for an autonomous mobile robot using differential encoder and a gyroscope. *Proceedings of the IEEE International Conference on Advanced Robotics*. 441-446.

Sala, P.L., R. Sim, A. Shokoufandeh, and S.J. Dickinson. 2004. Landmark selection for vision-based navigation. *Proceedings of the IEEE International Conference on Intelligent Robots and Systems*. Vol. 4, 3131-3138.

Schonberg, T., M. Ojala, J. Suomela, A. Torpo, and A. Halme. 1996. Positioning an autonomous off-road vehicle by using fused DGPS and inertial navigation. *International Journal of Syst. Sc*. Vol. 27 (8), 745-752.

Skewis, T., and V. Lumesly. 1994. Experiments with a mobile robot operating in a cluttered unknown environment. *International Journal of Robotic Systems*. Vol. 11 (4), 281-300.

Sugihara, K. 1988. Some location problems for robot navigation using a single camera. *Computer Vision, Graphics and Image Processing*. Vol. 42, 112-129.

Sutherland, K.T., and W.B. Thompson. 1993. Inexact navigation. *Proceedings of IEEE International Conference on Robotics and Automation.* Vol. 1, 1-7.

Vaganay, J., M.J. Aldon, and A. Fourinier. 1993. Mobile robot attitude estimation by fusion of inertial data. *Proceedings of the IEEE International Conference on Robotics and Automation*. Vol. 1, 277-282.

Yamauchi, B. 1996. Mobile robot localization in dynamic environments using dead reckoning and evidence grids. *IEEE Conference on Robotics and Automation*. Vol. 2, 1401-1406